RETROSPECTIVE ILLUMINATION CORRECTION OF RETINAL FUNDUS IMAGES FROM GRADIENT DISTRIBUTION SPARSITY

Yuanjie Zheng[1], Brian Vanderbeek[2], Rui Xiao[3], Ebenezer Daniel[2], Dwight Stambolian[2], Maureen Maguire[2], Joan O'Brien[2], James Gee[1]

[1]Department of Radiology, University of Pennsylvania, Philadelphia, PA

[2]Department of Ophthalmology, University of Pennsylvania, Philadelphia, PA

[3]Department of Biostatistics and Epidemiology, University of Pennsylvania, Philadelphia, PA

ABSTRACT

We present a novel technique for retrospective illumination correction of retinal fundus images from the sparsity property of image gradient distribution. It can automatically estimate the illumination inhomogeneity given an arbitrary retinal fundus image. Experimental results on 665 high resolution fundus images show both the efficiency of our algorithm on illumination correction and its high value on improving the accuracy of blood-vessel segmentation.

1. INTRODUCTION

Retinal photography with advanced fundus cameras is becoming a must in optometric practices and ophthalmologic clinics. The produced digital retinal images can be used in computer aided diagnosis (CAD) of age-related macular degeneration (AMD), glaucoma, diabetic retinopathy, etc. Improper scene illumination and the spherical geometry of the eye can both introduce severe distortion into the retinal images, which is typically perceived as smooth intensity variations across the image. Correction of this illumination inhomogeneities (also called bias field) is highly desirable in obtaining high-quality results in many image applications including image stitching, image matching, image segmentation, etc.

Different techniques have been proposed to correct the illumination inhomogeneity in retinal fundus images [1] or other medical images. The earliest work used prospective methods that rely on imaging uniform phantoms [2]. These methods can be considered as the ground truth but are not often applicable in practice because the fundus camera or imaging machine is not always available. Recent illumination correction techniques focus on retrospective methods which are dependent on the image directly and free from the requirement of fundus camera or imaging machine. They can be classified as filtering methods [3] by estimating the bias field with the low frequencies of fundus images, surface fitting based methods based on the intensities of major tissues or the image gradients [4], segmentation based methods performed by repeating two processes of image segmentation and bias field fitting [5], and image intensity histogram based methods through maximizing the high frequency of the image intensity distribution [6] or minimizing the image entropy [7].

In this paper, we propose to use the sparsity property of image gradient distribution in illumination correction of retinal fundus image. The sparse image gradient distribution is typically characterized by its sharp-peaked, heavy-tailed and symmetric shape, which has attracted much interest in computer vision and computer graphics [8, 9, 10]. By maximizing the sparseness of image gradient distribution of a given single retinal image, our algorithm can accurately estimate the latent bias field. We believe that like the high frequency of the image intensity distribution [6] or the image entropy [7], the sparsity of image gradient distribution will become an important measurement in estimating image bias field.

2. METHOD

We assume a given 2D retinal image Z is the product of the illumination inhomogeneity free image I and a bias field B, as expressed below

$$Z(i,j) = I(i,j)B(i,j), \tag{1}$$

where (i,j) index pixel in the image, and if M and N represent the total numbers of rows and columns, respectively, we have $1 \leq i \leq M$ and $1 \leq j \leq N$.

The goal of illumination correction is to estimate B in Eq. (1) for each pixel. This is obviously a classic ill-posed problem because the number of unknowns (I and B) is twice the number of equations. To make it solvable, we need to add constraints on both I and B.

Instead of computing B directly, we solve for its logarithm. Let $\mathcal{Z} = \ln Z$, $\mathcal{I} = \ln I$, and $\mathcal{B} = \ln B$, we have

$$\mathcal{Z}(i,j) = \mathcal{I}(i,j) + \mathcal{B}(i,j). \tag{2}$$

Denoting the gradients of $\mathcal{Z}$, $\mathcal{I}$, and $\mathcal{B}$ for each pixel (i,j) with $\psi^{\mathcal{Z}}(i,j)$, $\psi^{\mathcal{I}}(i,j)$, and $\psi^{\mathcal{B}}(i,j)$, respectively, we have

$$\psi^{\mathcal{Z}}(i,j) = \psi^{\mathcal{I}}(i,j) + \psi^{\mathcal{B}}(i,j). \tag{3}$$

Given an image $\mathcal{Z}$, we find a maximum a posteriori (MAP) solution to $\mathcal{B}$. Using Bayes' rule, this amounts to

solving the following optimization problem

$$\mathcal{B} = \arg\max_{\mathcal{B}} P(\mathcal{B}|\mathcal{Z}) \propto \arg\max_{\mathcal{B}} P(\mathcal{Z}|\mathcal{B})P(\mathcal{B}). \quad (4)$$

In Eq. (4), $P(\mathcal{Z}|\mathcal{B})$ and $\mathcal{B}$ are determined by two prior-knowledge: the sparsity property of image gradient distribution of $\mathcal{I}$ and smoothness of the bias field, respectively.

2.1. Gradient Distribution Sparsity

To compute $P(\mathcal{Z}|\mathcal{B})$, we impose sparsity on the image gradient distribution of the bias free image $\mathcal{I} = \mathcal{Z} - \mathcal{B}$ as below

$$P(\mathcal{Z}|\mathcal{B}) = P\left(\psi^{\mathcal{I}}\right) = e^{-\left|\psi^{\mathcal{I}}\right|^{\alpha_g}}, \quad (5)$$

where $0 < \alpha_g < 1$ controls the sparsity degree of the gradient distribution. Value of α_g in Eq. (5) is fit with a series of bias free retinal fundus images using the maximum likelihood criterion (details omitted for economy).

From Eq. (3), we have

$$\psi^{\mathcal{I}}(i,j) = \psi^{\mathcal{Z}}(i,j) - \psi^{\mathcal{B}}(i,j) \ . \quad (6)$$

Substituting Eq. (6) into Eq. (5) yields

$$P(\mathcal{Z}|\mathcal{B}) = e^{-\sum_{(i,j)}\left|\psi^{\mathcal{Z}}(i,j)-\psi^{\mathcal{B}}(i,j)\right|^{\alpha_g}}. \quad (7)$$

2.2. Parametric Model of Bias Field

The bias field $\mathcal{B}$ is pre-known to be smooth and can be represented by different parametric models, e.g. the cubic B-splines and the bivariate polynomial. We choose the bivariate polynomial for its efficiency [4], for which the model in degree D (e.g. 4) is expressed as

$$\mathcal{B}(i,j) = \sum_{t=0}^{D}\sum_{l=0}^{t} a_{t-l,l} x_{(i,j)}^{t-l} y_{(i,j)}^{l} \quad (8)$$

where $\{a_{t-l,l}\}$ are parameters of the model, and $x_{(i,j)}$ and $y_{(i,j)}$ are the x-axis and y-axis coordinates of pixel (i,j), respectively. Note that the number of elements in $\{a_{t-l,l}\}$ is $(D+1)(D+2)/2$.

Note that the bivariate polynomial model in a low degree only allows changes in low frequency and therefore already applies smoothness in the estimated bias field.

2.3. Object Function

The maximization of Eq. (4) becomes the the minimization of the below object function

$$\mathcal{O} = \sum_{(i,j)}\left|\psi^{\mathcal{Z}}(i,j) - \psi^{\mathcal{B}}(i,j)\right|^{\alpha_g} + \epsilon\sum_{t=0}^{D}\sum_{l=0}^{t} a_{t-l,l}^{\alpha_a}, \quad (9)$$

where ϵ takes a very small value (e.g. 0.00001). In Eq. (9), the sparse constraint on $\{a_{t-l,l}\}$ is applied in order to get a unique solution and accomplish adaptive specification on the smoothness degree of the resulting bias field.

The minimization of Eq. (9) does not have a closed-form solution because the exponents α_g and α_a are less than one. To solve it, most nonlinear optimization techniques can be directly applied, however, they would be very time-consuming and easy to be trapped into a local minimum considering the large number of unknowns in Eq. (9). To solve these difficulties, we employ the iteratively re-weighted least squares (IRLS) technique [11]. IRLS poses the optimization as a sequence of standard least squares problems, each using a weight factor based on the solution of the previous iteration. Specifically, at the kth iteration, the energy function using the new weight can be written as

$$\mathcal{O} = \sum_{(i,j)} w_k(i,j)\left(\psi^{\mathcal{Z}}(i,j) - \psi^{\mathcal{B}}(i,j)\right)^2 + \epsilon\sum_{t=0}^{D}\sum_{l=0}^{D-t} w'_k(t,l)a_{t,l}^2, \quad (10)$$

where weight $w_k(i,j)$ is computed in terms of the optimal $\mathcal{B}_{k-1}$ from the last iteration as

$$\begin{aligned} &w_k(i,j) = e^{-S_1}(1-e^{-S_2}),\\ &S_1 = \left|\psi^{\mathcal{Z}}(i,j) - \psi^{\mathcal{B}_{k-1}}(i,j)\right|, \quad S_2 = \alpha_g\left(S_1\right)^{\alpha_g - 1} \end{aligned} \quad (11)$$

and $w'_k(t,l)$ is computed by

$$w'_k(t,l) = e^{-|a_{t,l}|}\left(1 - e^{-\alpha_a|a_{t,l}|^{\alpha_a - 1}}\right). \quad (12)$$

2.4. Solution

To minimize Eq. (10), we rewrite $\psi^{\mathcal{Z}}$ and $\psi^{\mathcal{B}}$ as expressions of known values $\mathcal{Z}$ and unknown variables $\{a_{t,l}\}$, respectively. We will show that $\psi^{\mathcal{Z}}$ can be expressed concisely as the product of a Laplacian matrix L_ψ and $\mathcal{Z}$, and $\psi^{\mathcal{B}}$ can be simplified as a linear equation of $\{a_{t,l}\}$.

We first define the horizontal and vertical gradients of $\mathcal{Z}$. The horizontal gradient can be approximated with $\psi_x^{\mathcal{Z}}(i,j) = \frac{\mathcal{Z}(i,j)-\mathcal{Z}(i,j-1)}{\delta x}$ where δx is the horizontal resolution of the given image, while the vertical gradient is computed by $\psi_y^{\mathcal{Z}}(i,j) = \frac{\mathcal{Z}(i,j)-\mathcal{Z}(i-1,j)}{\delta y}$ where δy is the vertical resolution of the given image.

To define L_ψ, taking $\psi_x^{\mathcal{Z}}$ as an example, we define a Laplacian matrices [12] L_{ψ_x} in size $M \times N$ by $M \times N$. Using (u,v) to index the elements in L_{ψ_x}, we have

$$L_{\psi_x}(u,v) = \begin{cases} \frac{1}{\delta_x} & \text{if } u{=}v,\\ \frac{-1}{\delta_x} & \text{if } u \text{ and } v \text{ are associated},\\ 0 & \text{otherwise}, \end{cases} \quad (13)$$

where "u and v are associated" means that pixel v is used in the computation of image gradient at pixel u. Obviously, for each u, there is only one v associated. It also means that each row of L_ψ contains only two nonzero elements. Similarly, we

can define L_{ψ_y} for the vertical gradient. Then, we have

$$L_\psi = \left[\begin{array}{c} L_{\psi_x} \\ L_{\psi_y} \end{array} \right]. \quad (14)$$

The horizontal gradient of $\mathcal{B}$ (expressed by Eq. (8)) at pixel (i, j) is computed with

$$\psi_x^{\mathcal{B}}(i,j) = \frac{\mathcal{B}(i,j)-\mathcal{B}(i,j-1)}{\delta x} = \frac{1}{\delta x}\sum_{t=0}^{D}\sum_{l=0}^{D-t} a_{t,l}\left(x_{(i,j)}^t - x_{(i,j-1)}^t\right) y_{(i,j)}^l \quad (15)$$

which can be seen as a linear combination of the parameters $\{a_{t,l}\}$. We can concatenate $\{a_{t,l}\}$ to form a vertical vector $\bar{a}$. For pixel (i, j), all combination parameters in Eq. (15) can also be concatenated to a vertical vector $\bar{c}_{x(i,j)}$. Apparently, to an element $a_{t,l}$ in $\bar{a}$, the corresponding element in $\bar{c}_{x(i,j)}$ takes value $\frac{1}{\delta x}\left(x_{(i,j)}^t - x_{(i,j-1)}^t\right) y_{(i,j)}^l$. Then, Eq. (15) becomes

$$\psi_x^{\mathcal{B}}(i,j) = \bar{c}_{x(i,j)}^T \bar{a}. \quad (16)$$

Similarly, we have the following equation for the vertical gradient of $\mathcal{B}$:

$$\psi_y^{\mathcal{B}}(i,j) = \bar{c}_{y(i,j)}^T \bar{a}. \quad (17)$$

Combining Eq. (16) and Eq. (17) for all pixels, we have

$$\psi^{\mathcal{B}} = \left[\begin{array}{c} \psi_x^{\mathcal{B}} \\ \psi_y^{\mathcal{B}} \end{array} \right] = \left[\begin{array}{c} C_x \\ C_y \end{array} \right] \bar{a} = C\bar{a}, \quad (18)$$

where C_x and C_y are matrices for which the number of rows equals the number of pixels and their rows corresponding to pixel (i, j) are $\bar{c}_{x(i,j)}^T$ and $\bar{c}_{y(i,j)}^T$, respectively.

Substituting Eq. (14) and Eq. (18) into Eq. (10) yields

$$\mathcal{O} = \|W_k L_\psi \bar{\mathcal{Z}} - W_k C\bar{a}\|^2 + \epsilon\|W_k'\bar{a}\|^2, \quad (19)$$

where W_k and W_k' are diagonal matrices formed by the square root value of $w_k(i, j)$ and $w_k'(t, l)$ in Eq. (10), respectively, and $\bar{\mathcal{Z}}$ is a vertical vector composed of all $\mathcal{Z}$ values.

With the ridge regression (or Tikhonov regularization) method, Eq. (19) results in

$$\hat{\bar{a}} = \left(C^T W_k^T W_k C + \epsilon {W_k'}^T W_k'\right)^{-1} C^T W_k^T W_k L_\psi \bar{\mathcal{Z}}. \quad (20)$$

Matrix operations of Eq. (20) can be solved efficiently. Although the numbers of rows and columns of matrices L_ψ and W_k are all equal to the number of pixels, these two matrices are both sparse. Matrix C is non-sparse but the number of columns in C equals to the number of the parameters $\{a_{t,l}\}$ in the bivariate polynomial model, generally much smaller than the total number of pixels. Matrix W_k' is sparse and the number of rows and columns equals to the number of the parameters $\{a_{t,l}\}$.

3. RESULTS

The proposed illumination correction technique has been tested with both subjective assessment and objective evaluation on the DRIIL [1] database containing 165 high resolution fundus images, 30 images from the Gold Standard Database (GSD)[2] for Evaluation of Fundus Image Segmentation Algorithms, and our own database composed of 470 high resolution fundus images. In our experiments, the green channel of the fundus image is used in bias estimation.

Subjective assessment was performed through visual inspection on the bias corrected image and the estimated bias field by an experienced operator, as shown in Fig. 1. The image was labeled as a failed case if an improper bias estimation (e.g. bias effect not eliminated or even enhanced) is obtained. We find that our algorithm failed only for two images among the totally 665 test images. The failures were mainly caused by the brightness of optic disk and the uneven colors of certain pathology regions.

The objective evaluation was conducted by treating our bias correction algorithm as a preprocessing step of the blood-vessel segmentation with one of our previous works. The influence of the bias correction on the accuracy of blood-vessel segmentation is validated with two sets of image from the GSD database: 15 images of healthy subjects and 15 images of diabetic patients. The corresponding website provides manual segmentation by a bioengineering expert, which can be treated as a gold-standard for evaluation. The sensitivity, specificity and accuracy of segmentation were evaluated for each image with and without bias correction, as summarized in Tab. 1. From these results, we can see obvious improvements of blood-vessel segmentation benefited from the illumination correction with our algorithm.

4. CONCLUSION

We proposed a retrospective illumination correction technique which can automatically eliminate the bias field in retinal fundus images. Our technique is based on a new measurement - sparsity of image gradient distribution. Experiments on a large number of fundus images show the efficiency of our algorithm and the high value in improving the performances of blood-vessel segmentation algorithms.

Our future work includes elimination of the negative affect of the optic disk in bias correction and the validation on the value of our algorithm in retinal image registration and in creating retinal panoramic photos.

5. REFERENCES

[1] Libor Kubecka, Jiri Jan, and Radim Kolar, "Retrospective illumination correction of retinal images," *International Journal*

[1] http://projects.ubmi.feec.vutbr.cz/ophthalmo/drill/

[2] http://www5.informatik.uni-erlangen.de/research/data/fundus-images

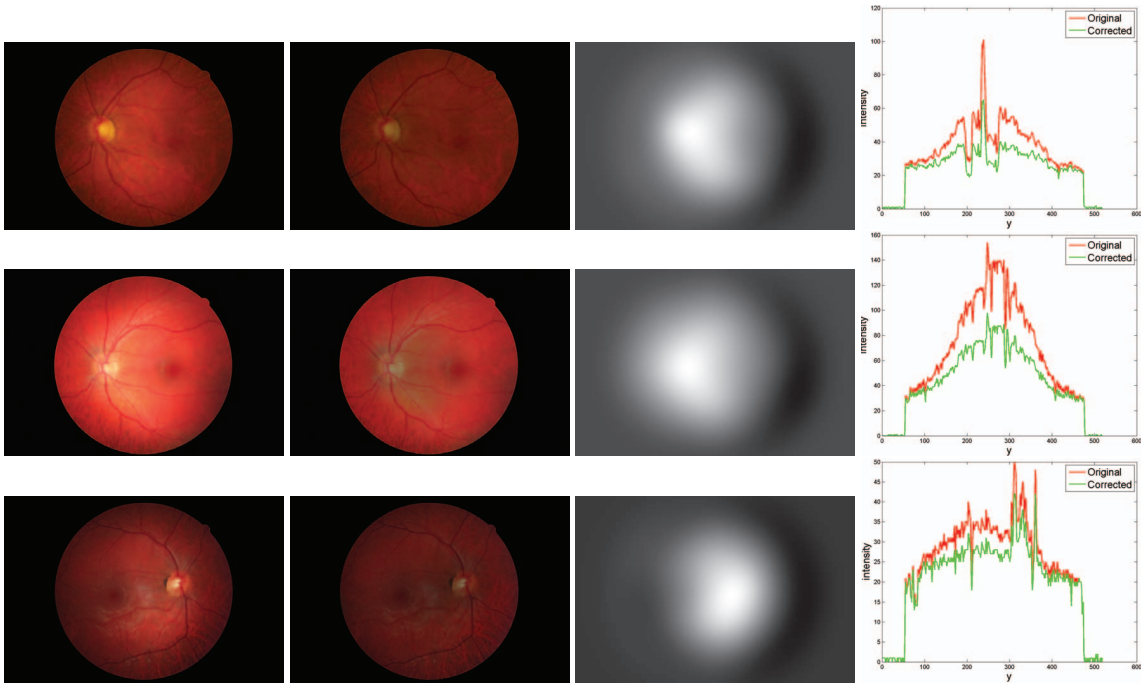


Fig. 1. Illumination correction results by our method. From left to right: original image, bias corrected image, the estimated bias field, and intensity profiles of the pixels on the center-vertical line of the original image (in red color) and the bias corrected image (in blue color).

	Healthy Subjects	Diabetic Patients
Sensitivity	**79.10**	74.21
	76.35	**76.88**
Specificity	**94.87**	**90.09**
	91.33	87.00
Accuracy	**94.61**	**92.72**
	92.58	90.47

Table 1. Quantitative evaluation of retinal blood-vessel segmentation with (upper value) and without (lower value) bias correction with our method, with higher values boldfaced.

of Biomedical Imaging, vol. 2010, pp. 1–10, 2010.

[2] L. Axel, J. Costantini, and J. Listerud, "Intensity correction in surface-coil mr imaging," *American Journal of Roentgenology*, vol. 148, pp. 418–420, 1987.

[3] B. H. Brinkmann, A. Manduca, and R. A. Robb, "Optimized homomorphic unshap masking for mr grayscale inhomogeneity correction," *IEEE Trans. on Medical Imaging*, vol. 17, pp. 161–171, 1998.

[4] Tolga Tasdizen, Elizabeth Jurrus, and Ross T. Whitaker, "Non-uniform illumination correction in transmission electron microscopy," in *MICCAI Workshop on Microscopic Image Analysis with Applications in Biology*, 2008.

[5] Dzung L. Pham and Jerry L. Prince, "Adaptive fuzzy segmentation of magnetic resonance images," *IEEE Transactions on Medical Imaging*, vol. 18, no. 9, pp. 737–752, 1999.

[6] Jogn G. Sled, Alex P. Zijdenbos, and Alan C. Evans, "A nonparametric method for automatic correction of intensity nonuniformity in MRI data," *IEEE Transactions on Medical Imaging*, vol. 17, no. 1, pp. 87–97, 1998.

[7] Martin Styner, Christian Brechbuhler, Gabor Szekely, and Guido Gerig, "Parametric estimate of intensity inhomogeneities applied to MRI," *IEEE Transactions on Medical Imaging*, vol. 19, pp. 153–165, 2000.

[8] Shaoting Zhang, Yiqiang Zhan, Maneesh Dewan, Junzhou Huang, Dimitris N. Metaxas, and Xiang Sean Zhou, "Towards robust and effective shape modeling: Sparse shape composition," *Medical Image Analysis*, vol. 16, no. 1, pp. 265 – 277, 2012.

[9] David L. Donoho and X. Huo, "Uncertainty principles and ideal atomic decomposition," *IEEE Transactions on Information Theory*, vol. 47, pp. 2845–2862, 2001.

[10] Emmanuel J. Candes, Michael B. Wakin, and Stephen P. Boyd, "Enhancing sparsity by reweighted l1 minimization," *Journal of Fourier Analysis and Applications*, vol. 14, pp. 877–905, 1999.

[11] P. Meer, *Robust techniques for computer vision*, pp. 107–190, Prentice-Hall, 2005.

[12] Dragos M. Cvetkovic, Michael Doob, Horst Sachs, and M. Cvetkovi&cacute, *Spectra of Graphs: Theory and Applications, 3rd Revised and Enlarged Edition*, New York: Wiley, 1998.